A Physics-Enhanced Neural Network for Estimating Longitudinal Dispersion Coefficient and Average Solute Transport Velocity in Porous Media

Yinquan Meng[1], Jianguo Jiang[1], Jichun Wu[2], and Dong Wang[2]

[1]School of Earth Sciences and Engineering, Nanjing University
[2]Nanjing University

April 12, 2024

Abstract

Dispersion coefficients and the average solute transport velocity are pivotal for groundwater solute transport modeling. Accurately and efficiently determining these parameters is challenging due to difficulties in directly correlating them with pore-space structure. To address this issue, we introduced the Physics-enhanced Convolutional Neural Network-Transformer (PhysenCT-Net), an innovative model designed to concurrently estimate the longitudinal dispersion coefficient and average solute transport velocity in three-dimensional porous media. PhysenCT-Net exhibited excellent predictive performance on unseen testing datasets and significantly reduced computational demands. Comprehensive evaluations confirmed its robust generalization across various flow conditions and pore structures. Notably, the longitudinal dispersion coefficient predictions closely align with established empirical relationships involving flow velocity, affirming the model's physical interpretability and potential to aid in simulating transport phenomena in porous media.

Hosted file

`Manuscript.docx` available at https://authorea.com/users/760442/articles/735962-a-physics-enhanced-neural-network-for-estimating-longitudinal-dispersion-coefficient-and-average-solute-transport-velocity-in-porous-media

A Physics-Enhanced Neural Network for Estimating Longitudinal Dispersion Coefficient and Average Solute Transport Velocity in Porous Media

Yinquan Meng[1], Jianguo Jiang[1*], Jichun Wu[1*], Dong Wang[1]

[1]Key Laboratory of Surficial Geochemistry of Ministry of Education, School of Earth Sciences and Engineering, Nanjing University, Nanjing, China

Corresponding author: Jianguo Jiang (jianguo.jiang@nju.edu.cn); Jichun Wu (jcwu@nju.edu.cn)

Key Points:

- Accurately predicting key parameters of the advection-dispersion equation for solute transport in porous media
- Developing direct mapping relationships between three-dimensional porous media images and parameters by the physics-enhanced neural network
- Network demonstrates exceptional prediction accuracy and generalization, providing parameters that align with an empirical formula

Abstract

Dispersion coefficients and the average solute transport velocity are pivotal for groundwater solute transport modeling. Accurately and efficiently determining these parameters is challenging due to difficulties in directly correlating them with pore-space structure. To address this issue, we introduced the Physics-enhanced Convolutional Neural Network-Transformer (PhysenCT-Net), an innovative model designed to concurrently estimate the longitudinal dispersion coefficient and average solute transport velocity in three-dimensional porous media. PhysenCT-Net exhibited excellent predictive performance on unseen testing datasets and significantly reduced computational demands. Comprehensive evaluations confirmed its robust generalization across various flow conditions and pore structures. Notably, the longitudinal dispersion coefficient predictions closely align with established empirical relationships involving flow velocity, affirming the model's physical interpretability and potential to aid in simulating transport phenomena in porous media.

Plain Language Summary

Advection-dispersion equation serves as the mathematical model for solute transport in aquifers and other porous media, with dispersion coefficients and average solute transport velocity (advective velocity) being key parameters. Typically, these are derived from optimization inversion of experimental data. Traditional pore-scale direct numerical simulation methods, while precise, demand considerable computational resources and time. To overcome these limitations, we developed PhysenCT-Net, a physics-enhanced neural network, aimed at simultaneously predicting the longitudinal dispersion coefficient and average solute transport velocity. The network integrates physical parameters such as molecular diffusion coefficient, Darcy velocity, and porosity into three-dimensional images of porous media through a convolutional neural network. The Transformer network then processes the high-dimensional data, with fully connected layers finalizing the concurrent prediction of both parameters. Direct simulations combined with an inversion technique calculate these parameters to establish the ground truth of the dataset. The trained PhysenCT-Net demonstrated outstanding predictive performance across various scenarios, proving its robustness. Transfer learning techniques further enhanced its generalization across different flow conditions and pore-space structures. Moreover, PhysenCT-Net represents a major advancement in physical interpretability for parameter prediction through deep learning methods.

1 Introduction

Precise modeling of solute dispersion within porous media holds significant relevance across various scientific and engineering disciplines, such as carbon dioxide sequestration, oil recovery, seawater intrusion into aquifers, and groundwater hydrology (Bear, 2013; Kamrava, Sahimi, et al., 2021; Sahimi, 2011; Xiong et al., 2020; Xiong et al., 2023). The transport of a conservative solute in porous media is governed by the advection-dispersion equation (ADE), wherein dispersion coefficients and average solute transport velocity (advective velocity in ADE) are pivotal parameters (Bear, 2013; Dentz et al., 2018; Lee et al., 2018). Dispersion coefficients cannot be directly measured and require be inferred or calibrated based on hypotheses related to observable characteristics (Abderrezzak et al., 2015; Ahsan, 2008). Previous studies have empirically or experimentally determined the longitudinal dispersion coefficient as a function of hydraulic and geometric parameters, such as Péclet number (Afshari et al., 2018; De Arcangelis

et al., 1986; Sahimi et al., 1986). Typically, the average advective velocity is assumed to be equivalent to the average fluid velocity; however, column experiments and pore-scale simulations have revealed discrepancies. This is because the solute distribution within pore spaces of porous media is not uniform (Darland & Inskeep, 1997; Rovey & Niemann, 2005; Zhang & Lv, 2009). Therefore, precise determination of the average advective velocity is essential for accurately simulating solute transport in porous media.

Pore-scale computational simulation methods, like pore network modelling (PNM), have been employed to investigate dispersion (Kamrava, Im, et al., 2021; Sahimi & Imdakm, 1988). However, PNM simplifies the pore space structure through inherent network approximations and treats the pore space as if it were composed of well-mixed entities, resulting in dispersive concentration profiles (Sadeghi et al., 2020; Yang et al., 2016). Consequently, other numerical simulation methods that directly model images of pore space, such as lattice Boltzmann method (LBM) or particle tracking, have increasingly been adopted to study dispersion in fluid flow (Bijeljic et al., 2011; Blunt et al., 2013; Hasan et al., 2020). Direct simulation methods can accurately compute macroscopic parameters of porous media, yet their substantial time and resource demands are significant limitations (Bedrunka et al., 2021; Kamrava, Im, et al., 2021). Therefore, a novel method that strikes a balance between efficiency and accuracy in parameter estimation is essential for effectively predicting solute transport processes.

In this letter, we introduce a physics-enhanced neural network, specifically designed to estimate longitudinal dispersion coefficient (D_L) and average solute transport velocity (u). The network leverages LBM and particle tracking simulations, combined with a parameter inversion approach, to provide a more efficient yet accurate solution for simulating transport phenomena in porous media.

Deep learning, or neural networks, have evolved as a superior alternative to traditional machine learning for analyzing complex system parameters (LeCun et al., 2015; LeCun et al., 1989; Vaswani et al., 2017). Notably, convolutional neural networks (CNNs) and Transformer networks have become leading architectures in computer vision and natural language processing, respectively, driving significant progress and forming the cornerstone of various deep learning applications (Devlin et al., 2018; He et al., 2017; He et al., 2016). CNNs excel in detecting local patterns and spatial information in images, making them ideal for linking the geometric features of porous media with their transport and physical properties, such as permeability and diffusivity (Elmorsy et al., 2022; Kamrava, Im, et al., 2021; Kamrava, Sahimi, et al., 2021; Rabbani et al., 2020; Tang et al., 2022). On the other hand, Transformer networks, with their self-attention mechanism, proficient in capturing long-range dependencies, enhancing feature extraction and generalization when combined with CNNs (Bai & Tahmasebi, 2022; Vaswani et al., 2017). This integrated CNN-Transformer approach achieves high accuracy with fewer parameters, proving advantageous in computational resource-limited settings and facilitating research on large-sized porous media (Meng et al., 2023). Moreover, the infusion of physical information into the network—permitting the direct assimilation of porous media's physical parameters during training—markedly elevates the model's predictive precision and its generalization capacity (Kamrava, Im, et al., 2021; Meng et al., 2023; Tang et al., 2022). In this letter, we propose the Physics-enhanced Convolutional Neural Network-Transformer (PhysenCT-Net), designed for the prediction of parameters D_L and u in large-sized ($200 \times 200 \times 1{,}000$ cubic voxels) porous media flows.

The structure of the letter is as follows: Section 2 introduces the numerical simulation methods of LBM and particle tracking, describes the data processing for training the PhysenCT-Net, and presents the network framework. In Section 3, we detail the research methodology of the PhysenCT-Net model, discussing the impact of varying data volumes, Péclet numbers, cementation and differences in particle size on the model's predictive and generalization capabilities. Section 4 summarizes and concludes the findings of the letter.

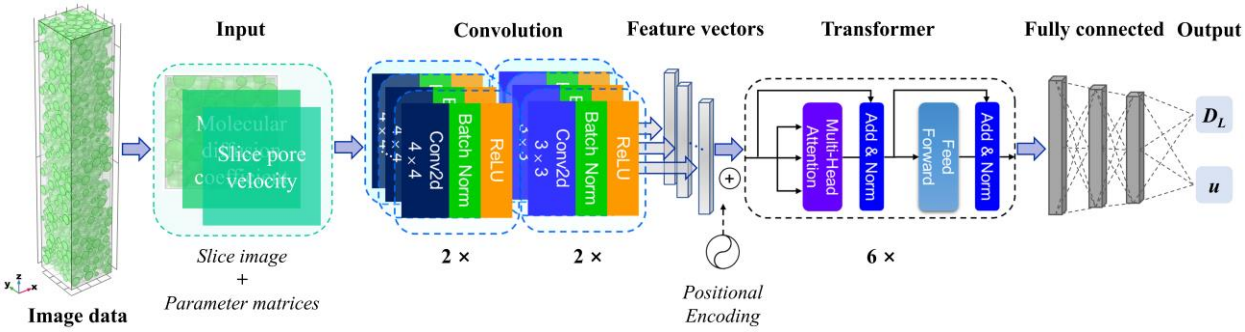

Figure 1. Schematic of the PhysenCT-Net

2 The Methodology

We first elucidate the methods for calculating the longitudinal dispersion coefficient D_L and average solute transport velocity u of the porous media, as well as the process of preparing and preprocessing data for PhysenCT-Net. Subsequently, we describe the framework of PhysenCT-Net.

2.1 Porous Media Generation and Parameter Calculation

We utilized the sedimentation-producing method (Batchelor, 1972; Pilotti, 1998) to fabricate three-dimensional (3D) porous media, subsequently modeling the flow field and solute transport by LBM and particle tracking method (Jiang & Wu, 2021; Mostaghimi et al., 2012).

The process of creating porous media via the sedimentation-producing method involves sequentially depositing spherical grains into a column. Each spherical grain starts at the top and descends freely until it reaches the column's bottom or lands on another grain. If the descending grain encounters another, it slides along the latter's surface until it finds a stable position, either at the bottom or in a state of minimum potential energy, thus preserving the porous medium's topological characteristics. This iterative process continues with subsequent grains. The spherical grains used in this method have diameters ranging from 0.4 to 1.2 mm, forming a porous medium with dimensions of 4 mm × 4 mm × 20 mm. Water flow is oriented along the column's long axis, with the porous medium's lateral boundaries defined as periodic to simulate an infinite system.

Generating 10,000 flow field samples for the dataset is computationally demanding. To efficiently manage the intricate boundaries within porous media, we employed the bounce-back scheme in LBM, specifically adopting the D3Q19 model to simulate pore-level flows. This model is formulated as:

$$f_i(x + e_i\Delta t, t + \Delta t) = f_i(x,t) + \frac{\Delta t}{\tau}\left[f_i^{eq}(x,t) - f_i(x,t)\right] \quad (1)$$

where $f_i(x,t)$ represents the density distribution function in the *i*th direction at discrete lattice point *x* and $f_i^{eq}(x,t)$ denotes the equilibrium distribution function, determined by the updated fluid velocities (Chen & Doolen, 1998).

For simulating solute molecule movement in porous media, we utilized the particle tracking method(Srinivasan et al., 2010). The solute's breakthrough curve at the porous media exit was calculated and then fitted by the ADE to determine the D_L and u. Solute transport within the porous media entails two dynamics: advective movement with water flow and random Brownian motion, which can be mathematically described as:

$$r(t+\Delta t) = r(t) + u\big(r(t)\big)\Delta t + 2\sqrt{D_m \Delta t}\,\xi \tag{2}$$

where u(r) indicates the flow velocity at the position r, D_m denotes molecular diffusion coefficient, and ξ represents a random variable conforming to a standard normal distribution.

The migration of conservative solutes in the porous media can be described by the ADE with the initial and boundary conditions (Van Genuchten, 1981):

$$\frac{\partial C}{\partial t} = D_L \frac{\partial^2 C}{\partial x^2} - u\frac{\partial C}{\partial x} \tag{3}$$

$$C(x,t)|_{t=0} = 0 \tag{4}$$

$$\left.\frac{\partial C}{\partial x}\right|_{x\to\infty} = \text{(finite)}\ (t \geq 0) \tag{5}$$

$$\left.\left(-D_L \frac{\partial C}{\partial x} + uC\right)\right|_{x=0} = uC_0 \tag{6}$$

where C is the solute concentration, C_0 the concentration of the injected solute, x the solute migration distance**,** u the average advective velocity, and D_L the longitudinal dispersion coefficient.

This mathematical model has an exact solution, which can be formulated as:

$$C(x,t) = C_0\left\{\frac{1}{2}erfc\left(\frac{x-ut}{2\sqrt{D_L t}}\right) + \sqrt{\frac{u^2 t}{\pi D_L}}exp\left[-\frac{(x-ut)^2}{4D_L t}\right] - \frac{1}{2}\left[1 + \frac{ux}{D_L} + \frac{u^2 t}{D_L}\right]exp\left(\frac{ux}{D_L}\right)erfc\left(\frac{x+ut}{2\sqrt{D_L t}}\right)\right\} \tag{7}$$

where the symbols are defined as above, *erfc* is the complementary error function.

For each sample of porous media, we designated two Darcy flow velocities and four molecular diffusion coefficients, resulting in four breakthrough curves $C(t)$ at the outlet. The D_L and u were precisely fitted via solute concentration analytical solutions (Eq. 7) and *SciPy* optimization inversion algorithm (Virtanen et al., 2020), respectively. The process minimizes the sum of squared residuals to align predicted concentration values $\hat{C}(t)$ closely with observed ones $C(t)$, thus accurately identifying optimal values for D_L and u.

2.2 Dataset Preparation

To enhance training of the neural network, we augmented the image dataset through vertical, horizontal, and diagonal flipping, effectively tripling the number of porous medium images

(Elmorsy et al., 2022). This strategy mitigated the issue of a single 3D image correlating with multiple D_L or u. We then constructed a dataset comprising 10,000 samples, with porosity (ε) of the 3D porous media ranging from 0.42 to 0.46. The Péclet number (Pe), defined as $Pe = vd/(\varepsilon D_m)$, where v represents the Darcy velocity, d the average grain diameter, varied between 12 and 12,000, with an average value of 806 and a standard deviation of 1227. The dimensions of the porous media images were $200\Delta x \times 200\Delta y \times 1{,}000\Delta z$, with $\Delta x = \Delta y = \Delta z = 20$ μm.

We constructed three-channel porous medium images infused with physical information entails the following steps: For each two-dimensional (2D) single-channel image within a sequence (depicting slices of a 3D porous medium), separate 2D parameter matrices for D_m and the slice pore velocity ($v_{sli} = v/\varepsilon_{sli}$), where ε_{sli} denotes the porosity of the 2D slice, respectively, are developed. The numerical values of these matrices are unified as D_m or v_{sli} and are then resized to align with the dimensions of the slice images. By integrating these two matrices with the original image along the channel axis, a 2D three-channel image with physical information is created, subsequently enhancing the entire sequence with physics.

2.3 The Neural Network Framework

The effectiveness of deep learning methods relies on the correct neural architecture and a sufficiently large dataset. In this letter, PhysenCT-Net primarily processes images of porous media infused with physical information through the CNN-Transformer architecture. A schematic of the PhysenCT-Net is depicted in Figure 1. The CNN comprises four convolutional layers, with the first two layers featuring 4 × 4 2D convolution kernels, a stride of 2, and padding of 1, and the number of channels in feature maps increasing sequentially from 12 to 24. The kernel size of the subsequent two convolutional layers is adjusted to 3 × 3, while maintaining a stride of 2 and padding of 1, with the channels in the feature maps escalating sequentially from 48 to 96. Following each convolutional operation, Batch Normalization (Ioffe & Szegedy, 2015) and the activation function of rectified linear unit (ReLU) (Nair & Hinton, 2010) are applied to enhance the network's non-linear representation capability. By setting up four convolutional layers, the three-channel (physics-enhanced) images of porous medium slices are transformed into 96-channel feature maps to represent their high-dimensional deep information. Subsequently, a fully connected layer compresses the feature map of each slice image into a feature vector with a dimensionality of 200. This same process is applied to each slice image of the porous medium, transforming the original 3D image into a sequence represented by a series of feature vectors. This sequence is then fed into the Transformer network as input.

The Transformer network, a deep learning model based on the multi-head self-attention mechanism, utilizes the mechanism to capture and learn the global dependencies within a sequence, thereby acquiring a long-term representation of the sequence (see Vaswani et al. (2017), for a comprehensive review of the terminology of the Transformer). We adopted the vanilla model proposed by Vaswani et al. (2017), which consists of six identical encoder layers, each containing two sublayers. The first sublayer, a multi-head attention layer, captures the relationships between elements (representing the compressed information of porous medium slice images) within the sequence. The second sublayer, a feed-forward fully connected layer, is employed for further feature extraction. Residual connections (He et al., 2016; Mo et al., 2019) and regularization operations between sublayers enhance the network's generalization ability and training stability. The Transformer network incorporates positional encoding into its input to capture the relative positional information of elements within the sequence; we employed

sinusoidal encoding (McAulay & Quatieri, 1995) for the purpose. After processing the input sequence, the Transformer network averages the outputs along the sequence length dimension, compressing them into a fixed-size vector. This vector then serves as the input to the fully connected layers following the Transformer network, with the output of the layers being the D_L and u.

3 The Computational Procedure and Results

Prior to training the neural network, standardizing parameter values is crucial to achieve consistency in data scale and distribution. Given the wide magnitude ranges for v and u (from 10^{-5} to 10^{-3} m/s), D_m (from 10^{-10} to 10^{-9} m²/s), and D_L (from 10^{-9} to 10^{-7} m²/s), we applied a logarithmic transformation to these parameters. Specifically, for v and u, a scaling factor of 10^5 is utilized preceding the logarithmic transformation to adjust the values to a more practical range. Similarly, for D_m and D_L, a scaling factor of 10^{10} is employed. This preprocessing step ensures the parameter values are uniformly scaled, facilitating the neural network's learning process.

During the training process of the neural network, we initially divided the dataset into a training set (80% of the data, totaling 8,000 samples) and a testing set (20% of the data, totaling 2,000 samples). The training set was further divided into a training subset and a validation subset at a ratio of 8:2. We employed the Adam optimizer (Kingma & Ba, 2014) with training epochs set to 30 and batch size to 32. The initial learning rate was set at 1e-4, with decay to 10%, 5%, and 2.5% of the initial rate at epochs 10, 20, and 25, respectively. The root mean square error (Chai & Draxler, 2014) was selected as the network's loss function. We ran the model five times and calculated the average coefficient of determination (R^2) values for D_L and u on the validation subset and testing set. The average R^2 for D_L on the validation subset was 0.9914, and for u was 0.9964; for the testing set, the average R^2 for D_L was 0.9913, and for u was 0.9962. The computational time for training dataset by LBM and particle tracking amounted to 10 million CPU seconds. While training the neural network required approximately 100,000 GPU seconds on four NVIDIA GeForce RTX 4090 GPUs. The direct prediction of D_L and u for the testing set by the trained PhysenCT-Net model required merely 1,600 GPU seconds. This represents a substantial improvement in computational efficiency, marked by several orders of magnitude, when compared to direct simulation approaches.

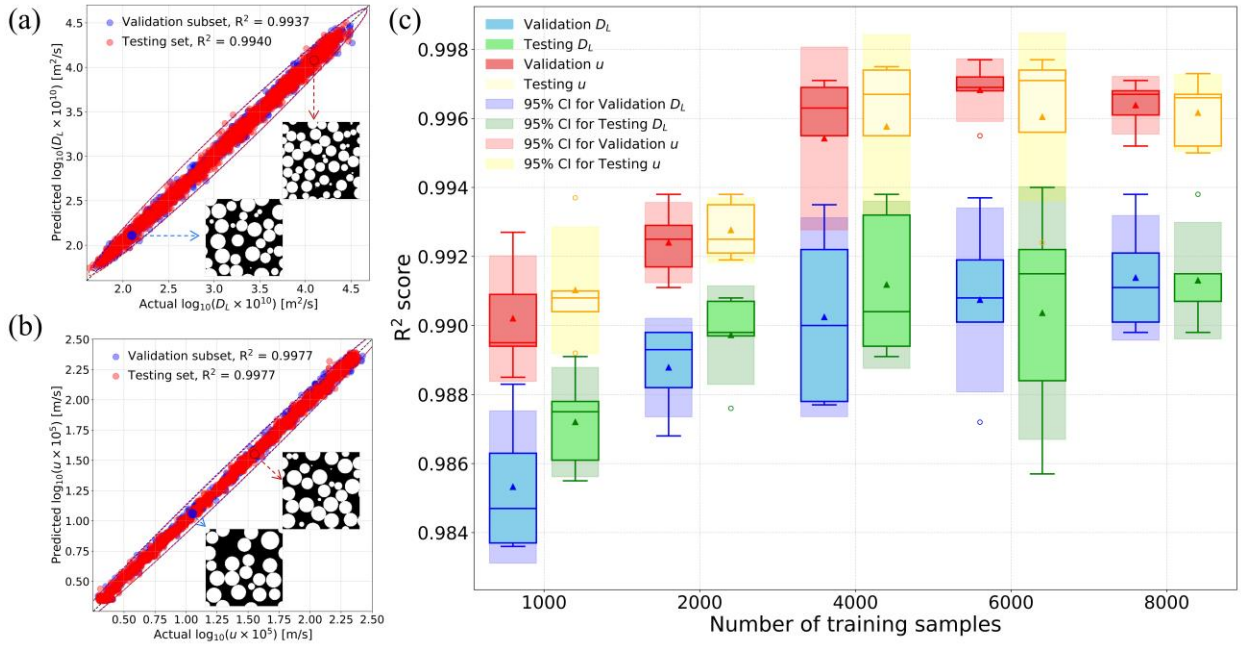

Figure 2. Performance of the PhysenCT-Net model on validation and testing sets: (a) and (b) showcase the optimal prediction results and porous medium structures in the dataset; (c) illustrates four box plots for each sample group, representing predictions of D_L and u for both validation and testing sets. Each box plot delineates the mean (triangle symbol), median (horizontal line within the box), outliers (dots), and the 95% confidence interval (shaded area) according to the *t*-distribution.

To examine the effect of training sample size on the predictive accuracy and generalization capability of the model, we modified the training dataset proportions to 10%, 20%, 40%, and 60% of the total data, while maintaining a constant testing set size. Each model variant, defined by its training sample size, underwent five rounds of training. Subsequently, we computed and illustrated the model's predictive accuracy (R^2) and its 95% confidence intervals employing the *t*-distribution methodology (Lange et al., 1989; Reich & Barai, 1999). As depicted in Figure 2, PhysenCT-Net exhibited remarkable precision and resilience. The model was capable of delivering precise predictions for unseen testing data with a minimal quantity of training samples (including instances where the training sample size was less than the testing sample size), with an observable enhancement in accuracy correlating with increased training data volume.

Bijeljic and Blunt (2006) employed the PNM method to investigate the relationship between hydrodynamic dispersion coefficients and *Pe*, while Mostaghimi et al. (2012) determined D_L as a function of the *Pe* through direct simulation. Instead of directly establishing a numerical relationship between *Pe* and D_L , we explored and evaluated the PhysenCT-Net model's capabilities to predict D_L and u with varying *Pe* conditions.

The PhysenCT-Net was set up with $Pe < 1{,}000$ (incorporating 7,552 samples) for training, partitioning the dataset into training and validation sets at an 8:2 ratio. The dataset for $Pe > 1{,}000$ conditions was designated as the testing set with 2,432 samples. The training approach was kept consistent, ensuring the dataset size strictly aligned with multiples of the batch size. The findings reveal that PhysenCT-Net (referenced in Figures 3a and 3b), with training conditions $Pe < 1{,}000$, yielded promising results on the validation set (totaling 1,504 samples), achieving R^2 values of

0.985 for D_L and 0.997 for u. However, its generalization capability on the unseen testing set (Pe > 1,000) was compromised, evidenced by R^2 values of 0.881 for D_L and 0.928 for u. To improve the model's generalization capacity, transfer learning methods were employed (Devlin et al., 2018; Yosinski et al., 2014). We refined the overall parameters of the trained models by utilizing 10% of the testing set samples, then proceeded to predict the remaining 90% of the testing set samples. During this phase, we adjusted the model's batch size to 16 and lowered the initial learning rate to 1e-5 to fit the smaller data sample size. The inset graphs at the lower right corners of Figures 3a and 3b display the model's predictions and R^2 values for 90% of the testing set, illustrating that transfer learning improved the model's generalization ability.

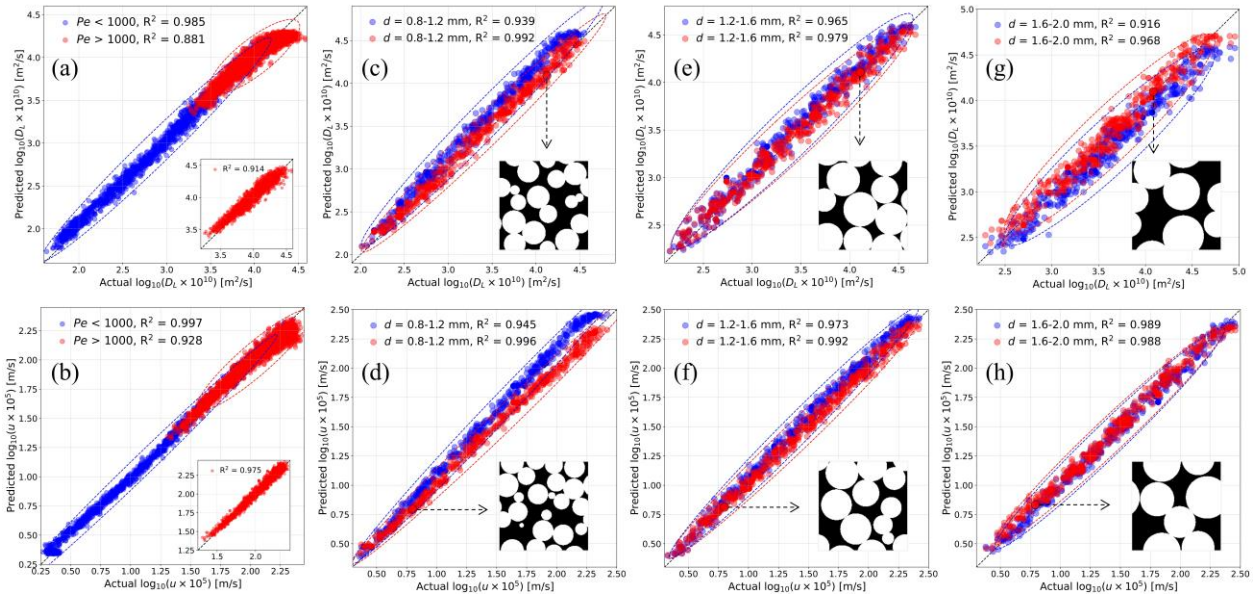

Figure 3. Model performance under different predicting conditions. (a) and (b) show the main graphs of each subfigure, illustrating direct predictions of the model on Pe < 1,000 (validation) and Pe > 1,000 (testing) datasets, respectively, while the inset graphs depict predictions for 90% of the testing datasets after transfer learning. (c)-(h) demonstrate model performance for predicting conditions with average grain diameters of 0.8 < d < 1.2 mm, 1.2 < d < 1.6 mm, and 1.6 < d < 2 mm. In the main graphs, blue dots represent direct predictions by the trained model on the dataset of 600 samples, while red dots indicate predictions for the remaining 90% by the retrained model after transfer learning. The inset graphs show the pore structure of the porous media in the corresponding datasets.

The primary dataset comprised 10,000 porous media with no cementation and grain sizes ranging from 0.4 to 1.2 mm. To evaluate the prediction performance of the trained models on cemented porous media with grain sizes between 0.8 and 2 mm, we developed three additional datasets. Each dataset contains 600 samples, featuring porosities spanning 0.37 to 0.39, 0.39 to 0.43, and 0.41 to 0.45, respectively. The model with the best generalization performance, as shown in Figures 2a and 2b, was adopted to directly predict D_L and u for each of these groups. The outcomes, represented by the blue scatter points in Figures 3c to 3h, confirmed the model's effectiveness in precisely estimating parameters for these unencountered porous media samples. Moreover, the application of transfer learning, represented by the red scatter points in the same figures, significantly enhanced the model's generalization ability. This finding highlights that

transfer learning, which involves fine-tuning model parameters with limited sample sizes, substantially strengthens the model's generalization capabilities, crucial for broader applicability. Leveraging the physics-enhanced neural network and transfer learning strategies discussed in this letter, we anticipate that the pretrained models will be adept at accurately estimating physical parameters across diverse porous media and under varied flow conditions.

During direct simulations, we assigned two Darcy flow velocities to each porous medium to calculate parameters D_L and u. In the training process of PhysenCT-Net, we applied three image transformations to each porous medium sample to prevent redundancy of input-output pairs in the deep learning dataset. Here, we created a unique dataset by assigning 256 different Darcy flow velocities to the same porous medium image samples while maintaining constant D_m. Six porous medium samples were selected for analysis. The trained PhysenCT-Net model reliably predicted an increment in the D_L as average fluid velocity increased. This pattern complies with the $D_L = \alpha_L \cdot u_{\text{avg}}^n + D_m$ empirical formula proposed by Cherry and Freeze (1979), where α_L denotes the longitudinal dispersivity and u_{avg} the average fluid velocity ($u_{\text{avg}} = v/\varepsilon$), validating the model's competency in providing parameter predictions consistent with physical principles. Such alignment emphasizes the model's proficiency in accurately capturing the fundamental physics governing solute transport in porous media.

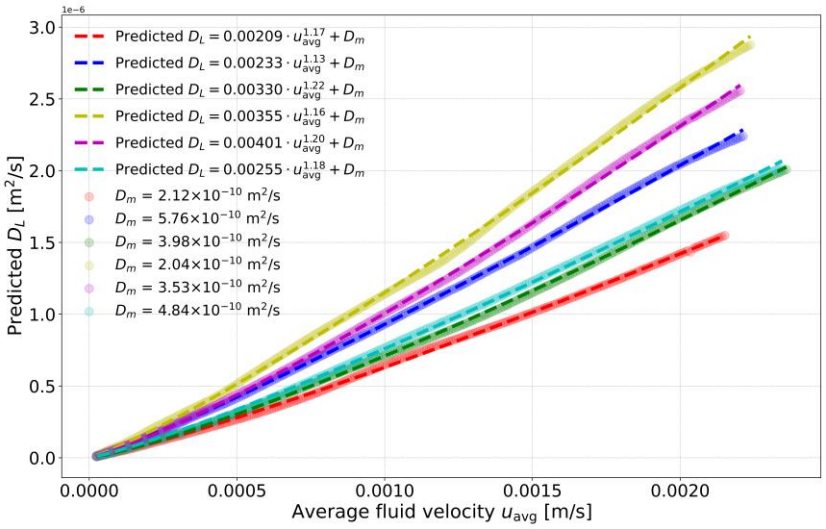

Figure 4. Predicted longitudinal dispersion coefficient versus average fluid velocity by the trained PhysenCT-Net model.

5 Conclusions

In this letter, we introduce the development of PhysenCT-Net, a significant advancement in utilizing neural networks to predict crucial solute transport parameters in porous media, such as the longitudinal dispersion coefficient and average solute transport velocity. The PhysenCT-Net methodology combines the precision of numerical simulation methods with the computational efficiency of deep learning technologies. It adeptly integrates three-dimensional images of porous media with pertinent physical parameters governing the dispersion process, showcasing robust performance and adherence to physical principles. Our study establishes the basis for future research that synergizes deep learning with direct pore-scale simulations, aiming for the rapid and precise determination of critical parameters to enhance the modeling of transport

phenomena in porous media and align computational predictions closely with real-world behaviors.

Data Availability Statement

Part of the dataset, codes, and trained models are accessible at https://doi.org/10.5281/zenodo.10858994 and can also be obtained from the corresponding author for detail upon reasonable request.

Acknowledgments

This study was jointly supported by the National Key Research and Development Program of China (grant no. 2022YFC3703700) and the National Natural Science Foundation of China (grant no. 41877177). We would also like to express our gratitude to the High-Performance Computing Center of Collaborative Innovation Center of Advanced Microstructures at Nanjing University for their assistance.

References

Abderrezzak, K. E. K., Ata, R., & Zaoui, F. (2015). One-dimensional numerical modelling of solute transport in streams: The role of longitudinal dispersion coefficient. *Journal of Hydrology, 527*, 978-989.

Afshari, S., Hejazi, S. H., & Kantzas, A. (2018). Longitudinal dispersion in heterogeneous layered porous media during stable and unstable pore-scale miscible displacements. *Advances in Water Resources, 119*, 125-141.

Ahsan, N. (2008). Estimating the coefficient of dispersion for a natural stream. *World Academy of Science, Engineering and Technology, 44*, 131-135.

Bai, T., & Tahmasebi, P. (2022). Characterization of groundwater contamination: A transformer-based deep learning model. *Advances in Water Resources, 164*.

Batchelor, G. (1972). Sedimentation in a dilute dispersion of spheres. *Journal of fluid mechanics, 52*(2), 245-268.

Bear, J. (2013). *Dynamics of fluids in porous media*: Courier Corporation.

Bedrunka, M. C., Wilde, D., Kliemank, M., Reith, D., Foysi, H., & Krämer, A. (2021). *Lettuce: Pytorch-based lattice boltzmann framework.* Paper presented at the High Performance Computing: ISC High Performance Digital 2021 International Workshops, Frankfurt am Main, Germany, June 24–July 2, 2021, Revised Selected Papers 36.

Bijeljic, B., & Blunt, M. J. (2006). Pore-scale modeling and continuous time random walk analysis of dispersion in porous media. *Water Resources Research, 42*(1).

Bijeljic, B., Mostaghimi, P., & Blunt, M. J. (2011). Signature of non-Fickian solute transport in complex heterogeneous porous media. *Physical Review Letters, 107*(20), 204502.

Blunt, M. J., Bijeljic, B., Dong, H., Gharbi, O., Iglauer, S., Mostaghimi, P., et al. (2013). Pore-scale imaging and modelling. *Advances in Water Resources, 51*, 197-216.

Chai, T., & Draxler, R. R. (2014). Root mean square error (RMSE) or mean absolute error (MAE)?–Arguments against avoiding RMSE in the literature. *Geoscientific model development, 7*(3), 1247-1250.

Chen, S., & Doolen, G. D. (1998). Lattice Boltzmann method for fluid flows. *Annual review of fluid mechanics, 30*(1), 329-364.

Cherry, J. A., & Freeze, R. A. (1979). *Groundwater*: Englewood Cliffs, NJ: Prentice-Hall.

Darland, J. E., & Inskeep, W. P. (1997). Effects of pore water velocity on the transport of arsenate. *Environmental science & technology, 31*(3), 704-709.

De Arcangelis, L., Koplik, J., Redner, S., & Wilkinson, D. (1986). Hydrodynamic dispersion in network models of porous media. *Physical Review Letters, 57*(8), 996.

Dentz, M., Icardi, M., & Hidalgo, J. J. (2018). Mechanisms of dispersion in a porous medium. *Journal of fluid mechanics, 841*, 851-882.

Devlin, J., Chang, M.-W., Lee, K., & Toutanova, K. (2018). Bert: Pre-training of deep bidirectional transformers for language understanding. *arXiv preprint arXiv:1810.04805*.

Elmorsy, M., El-Dakhakhni, W., & Zhao, B. (2022). Generalizable Permeability Prediction of Digital Porous Media via a Novel Multi-Scale 3D Convolutional Neural Network. *Water Resources Research, 58*(3).

Hasan, S., Niasar, V., Karadimitriou, N. K., Godinho, J. R., Vo, N. T., An, S., et al. (2020). Direct characterization of solute transport in unsaturated porous media using fast X-ray synchrotron microtomography. *Proceedings of the National Academy of Sciences, 117*(38), 23443-23449.

He, K., Gkioxari, G., Dollár, P., & Girshick, R. (2017). *Mask r-cnn.* Paper presented at the Proceedings of the IEEE international conference on computer vision.

He, K., Zhang, X., Ren, S., & Sun, J. (2016). *Deep residual learning for image recognition.* Paper presented at the Proceedings of the IEEE conference on computer vision and pattern recognition.

Ioffe, S., & Szegedy, C. (2015). *Batch normalization: Accelerating deep network training by reducing internal covariate shift.* Paper presented at the International conference on machine learning.

Jiang, J., & Wu, J. (2021). Interpolation for the lattice-Boltzmann method to simulate colloid transport in porous media. *Physical Review E, 103*(5), 053309.

Kamrava, S., Im, J., Barros, F. P. J., & Sahimi, M. (2021). Estimating Dispersion Coefficient in Flow Through Heterogeneous Porous Media by a Deep Convolutional Neural Network. *Geophysical Research Letters, 48*(18).

Kamrava, S., Sahimi, M., & Tahmasebi, P. (2021). Simulating fluid flow in complex porous materials by integrating the governing equations with deep-layered machines. *npj Computational Materials, 7*(1), 127.

Kingma, D. P., & Ba, J. (2014). Adam: A method for stochastic optimization. *arXiv preprint arXiv:1412.6980*.

Lange, K. L., Little, R. J., & Taylor, J. M. (1989). Robust statistical modeling using the t distribution. *Journal of the American Statistical Association, 84*(408), 881-896.

LeCun, Y., Bengio, Y., & Hinton, G. (2015). Deep learning. *nature, 521*(7553), 436-444.

LeCun, Y., Boser, B., Denker, J. S., Henderson, D., Howard, R. E., Hubbard, W., & Jackel, L. D. (1989). Backpropagation applied to handwritten zip code recognition. *Neural computation, 1*(4), 541-551.

Lee, J., Rolle, M., & Kitanidis, P. K. (2018). Longitudinal dispersion coefficients for numerical modeling of groundwater solute transport in heterogeneous formations. *Journal of Contaminant Hydrology, 212*, 41-54.

McAulay, R. J., & Quatieri, T. (1995). Sinusoidal coding. *Speech coding and synthesis, 4*, 121-173.

Meng, Y., Jiang, J., Wu, J., & Wang, D. (2023). Transformer-based deep learning models for predicting permeability of porous media. *Advances in Water Resources, 179*, 104520.

Mo, S., Zhu, Y., Zabaras, N., Shi, X., & Wu, J. (2019). Deep Convolutional Encoder-Decoder Networks for Uncertainty Quantification of Dynamic Multiphase Flow in Heterogeneous Media. *Water Resources Research, 55*(1), 703-728.

Mostaghimi, P., Bijeljic, B., & Blunt, M. J. (2012). Simulation of flow and dispersion on pore-space images. *SPE Journal, 17*(04), 1131-1141.

Nair, V., & Hinton, G. E. (2010). *Rectified linear units improve restricted boltzmann machines.* Paper presented at the Proceedings of the 27th international conference on machine learning (ICML-10).

Pilotti, M. (1998). Generation of realistic porous media by grains sedimentation. *Transport in Porous Media, 33*, 257-278.

Rabbani, A., Babaei, M., Shams, R., Wang, Y. D., & Chung, T. (2020). DeePore: A deep learning workflow for rapid and comprehensive characterization of porous materials. *Advances in Water Resources, 146*.

Reich, Y., & Barai, S. (1999). Evaluating machine learning models for engineering problems. *Artificial Intelligence in Engineering, 13*(3), 257-272.

Rovey, C. W., & Niemann, W. L. (2005). Do Conservative Solutes Migrate at Average Pore-Water Velocity? *Groundwater, 43*(1), 52-62.

Sadeghi, M. A., Agnaou, M., Barralet, J., & Gostick, J. (2020). Dispersion modeling in pore networks: A comparison of common pore-scale models and alternative approaches. *J Contam Hydrol, 228*, 103578. https://www.ncbi.nlm.nih.gov/pubmed/31767229

Sahimi, M. (2011). *Flow and transport in porous media and fractured rock: from classical methods to modern approaches*: John Wiley & Sons.

Sahimi, M., Hughes, B. D., Scriven, L., & Davis, H. T. (1986). Dispersion in flow through porous media—I. One-phase flow. *Chemical Engineering Science, 41*(8), 2103-2122.

Sahimi, M., & Imdakm, A. (1988). The effect of morphological disorder on hydrodynamic dispersion in flow through porous media. *Journal of Physics A: Mathematical and General, 21*(19), 3833.

Srinivasan, G., Tartakovsky, D. M., Dentz, M., Viswanathan, H., Berkowitz, B., & Robinson, B. A. (2010). Random walk particle tracking simulations of non-Fickian transport in heterogeneous media. *Journal of Computational Physics, 229*(11), 4304-4314.

Tang, P., Zhang, D., & Li, H. (2022). Predicting permeability from 3D rock images based on CNN with physical information. *Journal of Hydrology, 606*.

Van Genuchten, M. T. (1981). Analytical solutions for chemical transport with simultaneous adsorption, zero-order production and first-order decay. *Journal of Hydrology, 49*(3-4), 213-233.

Vaswani, A., Shazeer, N., Parmar, N., Uszkoreit, J., Jones, L., Gomez, A. N., et al. (2017). Attention is all you need. *Advances in neural information processing systems, 30*.

Virtanen, P., Gommers, R., Oliphant, T. E., Haberland, M., Reddy, T., Cournapeau, D., et al. (2020). SciPy 1.0: fundamental algorithms for scientific computing in Python. *Nature methods, 17*(3), 261-272.

Xiong, G., An, Q., Fu, T., Chen, G., & Xu, X. (2020). Evolution analysis and environmental management of intruded aquifers of the Dagu River Basin of China. *Science of the Total Environment, 719*, 137260.

Xiong, G., Zhu, X., Wu, J., Liu, M., Yang, Y., & Zeng, X. (2023). Seawater intrusion alters nitrogen cycling patterns through hydrodynamic behavior and biochemical reactions: Based on Bayesian isotope mixing model and microbial functional network. *Science of the Total Environment, 867*, 161368.

Yang, X., Mehmani, Y., Perkins, W. A., Pasquali, A., Schönherr, M., Kim, K., et al. (2016). Intercomparison of 3D pore-scale flow and solute transport simulation methods. *Advances in Water Resources, 95*, 176-189.

Yosinski, J., Clune, J., Bengio, Y., & Lipson, H. (2014). How transferable are features in deep neural networks? *Advances in neural information processing systems, 27*.

Zhang, X., & Lv, M. (2009). The nonlinear adsorptive kinetics of solute transport in soil does not change with pore-water velocity: Demonstration with pore-scale simulations. *Journal of Hydrology, 371*(1-4), 42-52.